

# Effect of Whole Body Parameters on Knee Joint Biomechanics

## Implications for ACL Injury Prevention During Single-Leg Landings

Sara Sadeqi,\*† PhD, Grant E. Norte,‡ PhD, AT, ATC, Amanda Murray,‡ PhD, PT, DPT, Deniz U. Erbulut,† PhD, and Vijay K. Goel,† PhD Investigation performed at the University of Toledo, Toledo, Ohio, USA

**Background:** Previous studies have examined the effect of whole body (WB) parameters on anterior cruciate ligament (ACL) strain and loads, as well as knee joint kinetics and kinematics. However, articular cartilage damage occurs in relation to ACL failure, and the effect of WB parameters on ACL strain and articular cartilage biomechanics during dynamic tasks is unclear.

**Purposes:** (1) To investigate the effect of WB parameters on ACL strain, as well as articular cartilage stress and contact force, during a single-leg cross drop (SLCD) and single-leg drop (SLD). (2) To identify WB parameters predictive of high ACL strain during these tasks.

Study Design: Descriptive laboratory study.

**Methods:** Three-dimensional motion analysis data from 14 physically active men and women were recorded during an SLCD and SLD. OpenSim was used to obtain their kinematics, kinetics, and muscle forces for the WB model. Using these data in kinetically driven finite element simulations of the knee joint produced outputs of ACL strains and articular cartilage stresses and contact forces. Spearman correlation coefficients were used to assess relationships between WB parameters and ACL strain and cartilage biomechanics. Moreover, receiver operating characteristic curve analyses and multivariate binary logistic regressions were used to find the WB parameters that could discriminate high from low ACL strain trials.

**Results:** Correlations showed that more lumbar rotation away from the stance limb at peak ACL strain had the strongest overall association ( $\rho$  = 0.877) with peak ACL strain. Higher knee anterior shear force ( $\rho$  = 0.895) and lower gluteus maximus muscle force ( $\rho$  = 0.89) at peak ACL strain demonstrated the strongest associations with peak articular cartilage stress or contact force in  $\geq$ 1 of the analyzed tasks. The regression model that used muscle forces to predict high ACL strain trials during the dominant limb SLD yielded the highest accuracy (93.5%), sensitivity (0.881), and specificity (0.952) among all regression models.

**Conclusion:** WB parameters that were most consistently associated with and predictive of high ACL strain and poor articular cartilage biomechanics during the SLCD and SLD tasks included greater knee abduction angle at initial contact and higher anterior shear force at peak ACL strain, as well as lower gracilis, gluteus maximus, and medial gastrocnemius muscle forces.

**Clinical relevance:** Knowledge of which landing postures create a high risk for ACL or cartilage injury may help reduce injuries in athletes by avoiding those postures and practicing the tasks with reduced high-risk motions, as well as by strengthening the muscles that protect the knee during single-leg landings.

Keywords: knee; ACL injury; single-leg cross drop; neuromuscular intervention; motion analysis experiments; computational biomechanics

Anterior cruciate ligament (ACL) injuries are quite common among young athletes, with devastating professional, financial, and social consequences.<sup>22</sup> Proper execution of high-speed dynamic athletic maneuvers can help reduce injury rates. Neuromuscular interventions have shown

positive outcomes in injury reduction <sup>20,24,28</sup>; however, the overall number of ACL injuries continues to rise, indicating a need to develop task-specific guidelines tailored to different athletic tasks. Risk reduction programs have focused on techniques that can alter kinematics and kinetic parameters identified as contributors to an ACL injury, including high knee abduction angles and moments, <sup>25,34</sup> low knee flexion, <sup>43</sup> and high internal or external rotation of the tibia. <sup>34</sup> Yet, these loads and motions at the knee joint do not occur without coupled

The American Journal of Sports Medicine 2023;51(8):2098–2109
DOI: 10.1177/03635465231174899

motions of other body parts,<sup>50</sup> and a thorough understanding of the relationship between other joints' kinematics and knee joint biomechanics is crucial for developing a comprehensive training program.

Researchers have used various methods, including motion analysis experiments, musculoskeletal simulations, and finite element (FE) analyses, to gain information on the associations between muscle forces  $^{45}$  and kinematics (upper body,  $^{10,19}$  lower body,  $^{19}$  whole body [WB] $^{10,13,15,61}$ ) with knee joint biomechanics and ACL forces<sup>46</sup> during athletic tasks, such as those requiring single-leg landings. However, previous studies are limited in several ways that limit translation to injurious scenarios. First, the knee was modeled with limited degrees of freedom (DOF) in several studies, allowing only for flexion-extension, with other rotations and translations constrained as functions of flexion<sup>45</sup> or including just the 3 knee rotations, <sup>13,15</sup> which neglect anterior tibial translation. Yet, anterior tibial shear force secondary to increased translation is a known contributor to ACL strain and should not be ignored. Second, muscle forces were not included in several studies. 13,15 Although electromyography has been used to infer muscular contributions, such studies can report only surface muscle activations, which lack the ability to provide information on the role of the deep muscles in knee joint loading and, hence, ACL and cartilage biomechanics. Additionally, simplifying the ligament representations from the anatomic 3-dimensional geometries to 2-dimensional springs or modeling cartilage tissues as rigid structures limits the capability of existing FE studies in reporting tissue stress under various loading conditions. 41,61,62 Last, previous studies 10,13,15,61 that investigated the effect of WB kinematics on ACL injury mechanisms during dynamic tasks have rarely reported on the resulting effect on articular cartilage biomechanics. Cartilage damage often occurs concomitantly with ACL injury, highlighting the implications of understanding the effect of WB parameters on ACL and cartilage biomechanics relative to long-term joint health, given the higher risk for osteoarthritis in this population.

Among the many athletic tasks that may increase the risk for ACL injury, the single-leg cross drop (SLCD) has been identified as a suitable screening task because of the involvement of the trunk control challenge and its inherent multiplanar joint motions. <sup>14</sup> This task requires the individual to jump from 1 limb off a raised platform and to land on the opposite limb across the body. The kinetics and kinematics of the SLCD have been studied <sup>14</sup>; however, the effect of WB parameters on ACL strain and

cartilage biomechanics remains unclear for this task. The single-leg drop (SLD) has been evaluated in previous studies <sup>33,37,40</sup> and has served as a clinical screening tool, <sup>30</sup> given its ability to provide kinematics and kinetics information in the frontal plane, <sup>33</sup> such as hip and knee abduction angles and moments, and its ease of performance and assessment. <sup>40</sup>

Thus, the primary objective of this study was to investigate the effects of WB kinematics, kinetics, and muscle forces on ACL strain and articular cartilage biomechanics during 2 dynamic tasks of SLCD and SLD using methods both in vivo (motion analysis) and in silico (musculoskeletal and FE). To extend on previous investigations, we sought to model the knee with 5 DOF and account for the effect of lower body and lumbopelvic musculature when reporting values of ACL strain and articular cartilage stress and contact force. The secondary objective of the study was to identify the cutoff values of the WB parameters that are able to predict high ACL strain under each condition. On the basis of previous literature, <sup>10,13,45,61</sup> we hypothesized that participants at high risk for the ACL injury mechanism and ACL strain could be identified via several WB parameters, such as increased trunk lateral bending away from the stance limb, increased hip abduction, decreased ankle plantarflexion, lower force production of the lumbopelvic musculature, and higher quadriceps forces.

### **METHODS**

### Motion Capture Experiments

Fourteen young, physically active volunteers with no history of knee injury participated in this experiment (7 women and 7 men; mean  $\pm$  SD age, 23.64  $\pm$  2.65 years; height,  $1.74 \pm 0.08$  m; weight,  $68.52 \pm 8.75$  kg). The level of physical activity was described in 2 ways: the Tegner Activity Scale and the International Physical Activity Questionnaire (Appendix A, Table A1, available in the online version of this article). Leg dominance was determined as the limb that would be used to kick a ball. All participants filled out consent forms approved by the institutional review board. The weights, heights, and anthropometric data of the participants were measured. Warm-up exercises included walking on a treadmill at a self-selected pace for 5 minutes. The participants were then free to do any warm-up of their choice (eg, stretching and mobility). Marker setup (detailed in Appendix A, available online) con-

<sup>\*</sup>Address correspondence to Sara Sadeqi, PhD, Engineering Center for Orthopaedic Research Excellence (E-CORE), Departments of Bioengineering and Orthopaedic Surgery, University of Toledo, 2801 Bancroft St, Toledo, OH 43606, USA (email: sara.sadeqi@utoledo.edu).

<sup>&</sup>lt;sup>†</sup>Engineering Center for Orthopaedic Research Excellence (E-CORE), Departments of Bioengineering and Orthopaedic Surgery, University of Toledo, Toledo, OH, USA.

<sup>&</sup>lt;sup>†</sup>Motion Analysis and Integrative Neurophysiology Lab, Department of Exercise and Rehabilitation Sciences, College of Health and Human Services, University of Toledo, Toledo, Ohio, USA.

Submitted September 30, 2022; accepted March 17, 2023.

One or more of the authors has declared the following potential conflict of interest or source of funding: Developing and validating the finite element model for this study was partially funded by the National Institutes of Health (grant R01 AR0056259-05A1; funder 10.13039/100000002) and Center for Disruptive Musculoskeletal Innovations (CDMI). AOSSM checks author disclosures against the Open Payments Database (OPD). AOSSM has not conducted an independent investigation on the OPD and disclaims any liability or responsibility relating thereto.

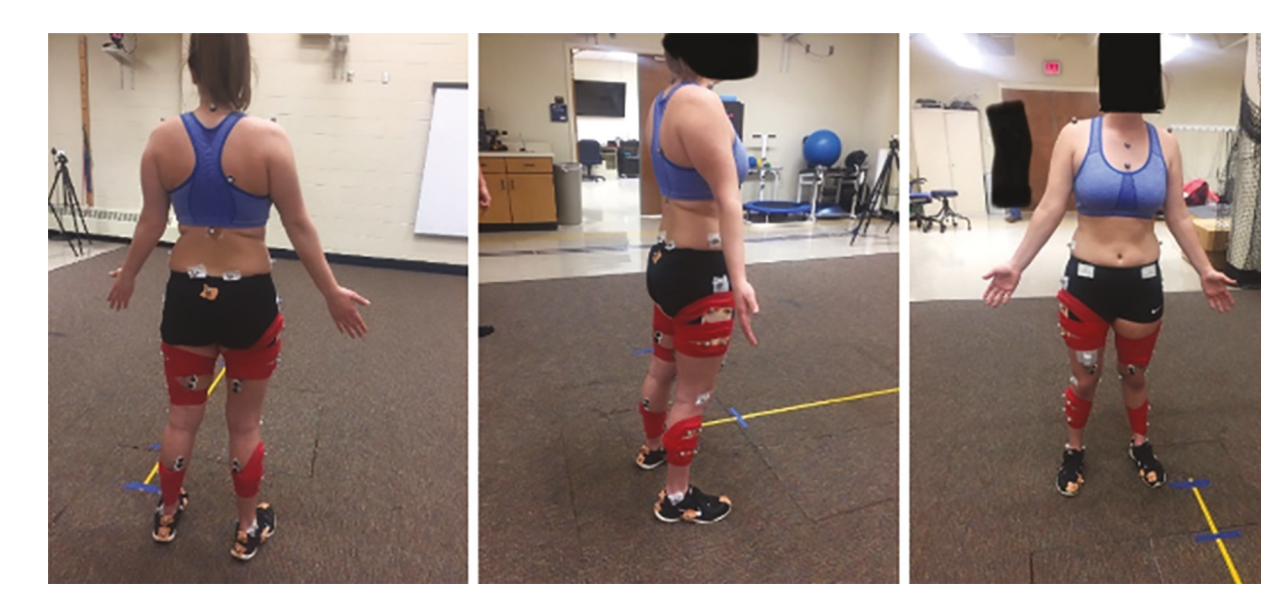


Figure 1. Marker arrangement on a female participant holding a static pose. For detailed views of marker placement, see Appendix A, Figure A1 (available online).

sisted of 46 reflective markers: 29 on the bony landmarks and 17 tracking markers (Figure 1). Participants wore spandex shorts and tops to reduce the relative marker skin motions. Marker trajectory data were collected for the static pose and the dynamic trials using 12 Raptor-E cameras (Motion Analysis Corp) with a sampling rate of 120 Hz. Cameras were calibrated before each participant's trial measurements. Participants were asked to perform an SLD and SLCD from a 30 cm-high platform and land on a force plate (Optima 464508-2000; Advanced Mechanics Technology) using their preferred postures on the dominant and nondominant limbs. Participants repeated the tasks as many times as required until 3 successful trials were recorded for each task. Successful trials were defined as landing with the whole stance foot on 1 force plate and holding the posture for a couple of seconds after landing. Raw marker data were then smoothed in Cortex (Motion Analysis) and postprocessed using Visual3D (Version 6.03.6; C-Motion). Visual3D was also used to obtain hip, knee, and ankle joint centers from the functional knee and anterior superior iliac spine trials.

Low-pass second-order Butterworth filters with cutoff frequencies of 6 and 12 Hz were used to filter kinematics and kinetics, respectively. The vertical component of the ground-reaction force was filtered with the cutoff frequency of 100 Hz to reserve the peak.<sup>53</sup>

### Musculoskeletal Modeling

Musculoskeletal simulations were performed in OpenSim software 12 (Version 4.0; OpenSim) using a full body model (Figure 2A) with 5 DOF at the knee joint 57 and a total of 31 DOF and 92 muscles in the model. A set of 46 markers was placed on the model according to the same protocol used to place them on the participants. The generic model was

scaled for each participant by using the recorded marker data of one's static pose. The scaling process was done in several iterations to achieve acceptable marker errors (root mean square <1 cm). Kinematics and kinetics were then calculated using the OpenSim inverse kinematics and inverse dynamics tools. OpenSim offers 2 optimization schemes for calculating muscle forces and activations: computed muscle control and static optimization. Computed muscle control accounts for passive muscle forces leading to higher muscle force values.<sup>51</sup> Static optimization was chosen in this study given that it was identified as the preferred method by other works<sup>39</sup> for its robustness and computational performance<sup>51</sup> and its usage popularity in reducing the redundancies while estimating muscle forces in human motion problems. 11 To ensure the acceptability of the musculoskeletal simulations, the magnitudes of residual forces and moments were checked to make sure that they were within the acceptable limits mentioned by the OpenSim documentation, typically <10 to 20 N and 75 N·m, respectively. Because residual forces and moments were small, a reduced residual analysis was not performed. Reserve torques used in the static optimizations were also kept <5% of the maximum net joint moments, as recommended by Hicks et al.<sup>27</sup>

The mean of 3 trials for each task was used as an input to the FE simulations. 6 Large variations among trials for 1 participant were seen in tibial rotation angles; therefore, the outlier trial was excluded in averaging for that specific participant.

### FE Simulations

One of the 4 previously validated knee FE models was selected for this study (23-year-old woman; height, 171.0 cm; weight, 60.3 kg; body mass index, 20.6) (Figure 2B). Details

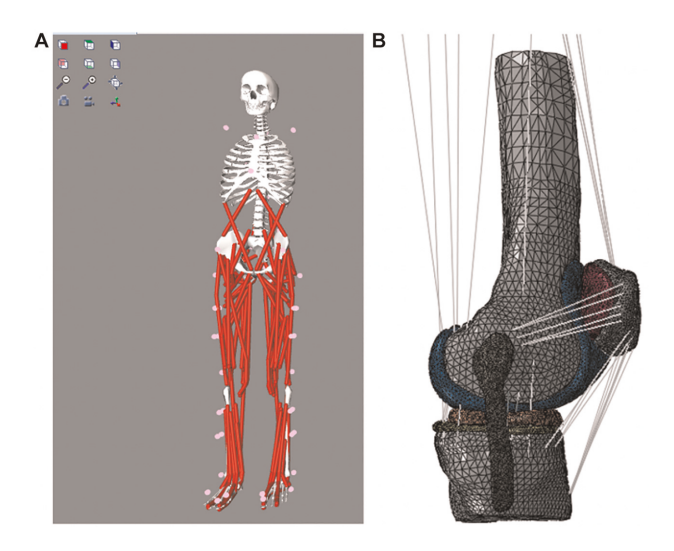


Figure 2. (A) Full-body OpenSim model with 5 degrees of freedom at the knee joint and the 46 markers (dots). (B) Knee joint finite element model. For more details on the finite element model components, see Appendix B, Figure B1 (available online).

on model development and validation were presented in our previous work. 17

FE simulations consisted of 2 steps (Figure 3). In the first step, the knee was flexed to the amount of flexion at initial contact (IC). Knee extensor forces (rectus femoris and vasti) and flexor forces (semimembranosus, semitendinosus, short and long heads of biceps femoris, sartorius, and gracilis) from the static optimizations were also applied in this step for preconditioning. The second step was simulating the landing phase for each jump. Noncontact ACL injury occurs during 30 to 100 milliseconds from the initial foot contact with the ground.<sup>26</sup> Therefore, the second step in the FE simulations replicated the 100 milliseconds from IC. The model was kinetically driven in this step, except for flexion. External loads from inverse dynamics-including knee abduction moment, internal tibial rotation moment, anterior tibial shear force, and knee compressive force from OpenSim inverse dynamics-were applied to the joint while the knee continued its flexion motion according to the angle from inverse kinematics. Similar to previous studies, 50% of the inverse dynamics moments were used in the FE analvses because it is believed that muscles and other soft tissue absorb half of these moments. 6,23 Some of the past studies have used 10% to 20% of these measured moments in their models. Those studies did not include the patella and patellar tendon<sup>58</sup> or used different parameters for the soft tissue, such as ligaments. In the current study, the patella and its attachments were present, and as shown by Halonen et al, <sup>23</sup> 50% would provide a more accurate representation in simulations. In both steps, the femur was fixed, and the kinetics and kinematics were applied to the joint center that was coupled to the tibia. Coordinate systems of the laboratory, musculoskeletal software, and FE were different. Appropriate transformations were used to apply the motions and loads in the correct direction. In this study, the outputs of

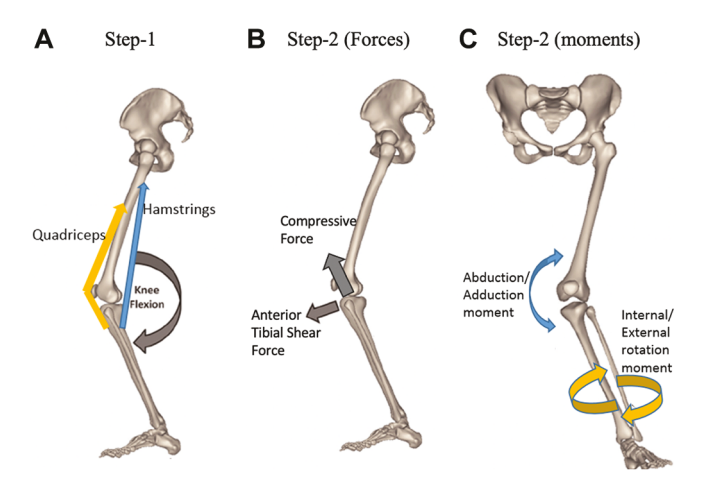


Figure 3. Steps of the finite element simulations. (A) Step 1 (preconditioning): the application of flexion angle, quadriceps, and hamstring forces. (B) Step 2 (forces): anterior tibial shear force and compressive force attributed to groundreaction force. (C) Step 2 (moments): internal/external tibial rotation moment and knee abduction/adduction moment.

the simulations consisted of peak relative ACL strain, peak stress, and peak contact force on the articular cartilage. Relative ACL strain<sup>18,55,63</sup> values were calculated and reported (ie, the strain relative to the preimpact length). The calculation of the ACL reference length was explained in our previous work.<sup>17</sup> Two points were selected on the anteromedial bundle of the ACL with approximately 10-mm distance, according to the in vitro strain gauge length in the study<sup>3</sup> used for our validation work.<sup>17</sup> The length after preconditioning the ligament in the first step of our current FE simulations was used as the reference length for strain calculations.

### Statistical Analysis

Open source Python<sup>42</sup> (Version 3.8.8; libraries and packages NumPy, Pandas, Matplotlib, and Seaborn) and SPSS (Version 28.0; IBM Corp) were used for data analysis and visualization. Kinetics and muscle forces were normalized for all statistical analyses. Moments were normalized by the product of participants' body mass (kilograms) × height (meters), forces by each participant's body weight (newton), and muscle forces by peak values (newton).

Spearman rho correlation coefficients (p) were used to assess the relationships between WB parameters and tissue biomechanics (ACL strain, articular cartilage stress, and articular cartilage contact force). Correlations were calculated separately for each of the 4 conditions: SLCD with nondominant stance leg (SLCD-N), SLCD with dominant stance leg (SLCD-D), SLD with nondominant stance leg (SLD-N), and SLD with dominant stance leg (SLD-D). The WB parameters entered in the correlation analyses included lumbar, hip, knee, and ankle kinetics and kinematics at 3 instances (peak values, values at IC, and values at peak ACL strain); muscle forces at peak ACL strain;

	TABLE 1	
Peak ACL Strain and Cartilage Stress and Cont	act Pressure Outputs From the FE	Simulations During SLCD and $SLD^a$
	I CD	CI D

	SI	LCD	S	LD
Peak Output	Dominant	Nondominant	Dominant	Nondominant
ACL strain, % Cartilage, MPa	$7.20\pm5.08$	$4.43\pm2.33$	$6.53\pm2.46$	$5.37\pm2.57$
Stress Contact pressure	$12.10 \pm 4.63$ $8.33 \pm 2.49$	$10.49 \pm 4.02 \\ 8.35 \pm 2.34$	$13.35 \pm 3.46$ $9.22 \pm 2.40$	$\begin{array}{c} 13.01\pm5.24 \\ 10.20\pm2.25 \end{array}$

<sup>&</sup>lt;sup>a</sup>Data are presented as mean ± SD. ACL, anterior cruciate ligament; FE, finite element; SLCD, single-leg cross drop; SLD, single-leg drop.

peak ground-reaction forces; peak ACL strains; and peak cartilage contact forces and stresses. A Benjamini-Hochberg correction was applied to all correlation coefficients to control for a 5% false discovery rate, and corrected coefficients were interpreted as weak (0 < $\rho$ < 0.4), moderate (0.4 <  $\rho$  < 0.7), or strong (0.70 <  $\rho$  < 1.0).

For predicting the high ACL strain trials and finding the cutoff values able to discriminate high versus low ACL strain, the continuous data of kinetics, kinematics, muscle forces, and ground-reaction forces for the 100-millisecond landing phase of each task were divided into 8-millisecond intervals for each participant, which led to 168 data points for each task (similar to an approach used by a previous study). 61 These trials were then divided into 2 categories for each task, based on the ACL strain value: high and low ACL strain trials. Trials with ACL strain values above the upper quartile were considered high ACL strain trials<sup>61</sup> for each condition. The total number of input parameters in each condition for kinematics, kinetics, and muscle force variables was 16, 20, and 49, respectively. Next, receiver operating characteristic (ROC) curve analyses and multivariate logistic regression analyses with the forward likelihood ratio method were performed in SPSS. To reduce data dimensionality and the number of input parameters for the logistic regressions, we initially performed 12 ROC analyses to identify the discriminative variables among kinematics, kinetics, muscle forces, and ground-reaction forces that were associated with ACL strain during each condition. The area under each ROC curve (AUC) and corresponding P values were used to determine the parameters that could have a diagnostic ability to discriminate between low and high ACL strain trials. Only statistically significant parameters from ROC analyses were kept for logistic regression, and when multicollinearity ( $\rho > 0.9$ ) was observed among them, just the one with the highest AUC was entered into the logistic regression. After logistic regression analyses were performed, only statistically significant variables were reported as the final discriminants. The AUC was used to categorize the discriminators of high ACL strain trials, and its strength was classified as  $\geq 0.9$  = excellent, 0.8-0.89 = good, 0.7-0.79 = acceptable, 0.5-0.69 = poor, and  $\le 0.5$  = no discrimination.<sup>54</sup> Overall accuracy, sensitivity, specificity, likelihood ratios, and statistical significance of each regression model were also reported. All analyses were evaluated at an alpha level of 0.05.

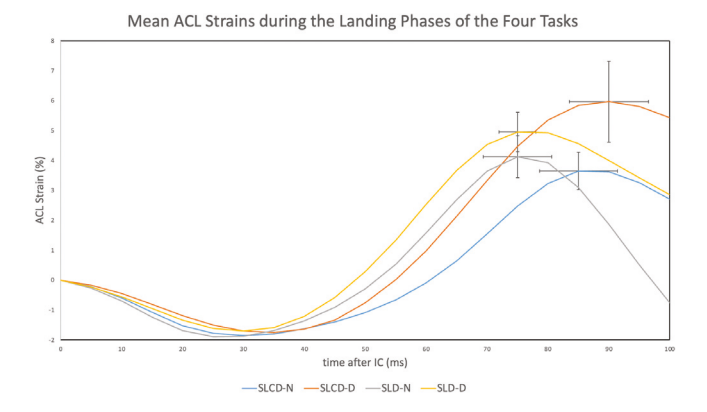


**Figure 4.** Anterior cruciate ligament (ACL) strain plots during the whole 100-millisecond landing phase for SLCD-D, SLCD-N, SLD-D, and SLD-N. Error bars show SE. D, dominant stance; IC, initial contact; N, nondominant stance; SLCD, single-leg cross drop; SLD, single-leg drop.

### **RESULTS**

### ACL Strain and Cartilage Biomechanics From FE

Table 1 shows the outputs of FE simulations. Peak stress values ranged from 6.47 to 18.25 MPa, and peak contact pressures were from 5.84 to 12.45 MPa. Peak contact forces up to 5.72 body weight and 4.56 body weight were seen on the medial and lateral tibial cartilage, respectively. Figure 4 shows ACL strain values during the 100 milliseconds after initial floor contact, averaged across the participants for each landing condition. Peak ACL strain occurred at 90, 85, 75, and 75 milliseconds after initial floor contact for SLCD-D, SLCD-N, SLD-D, and SLD-N, respectively.

### Correlation Between WB Parameters and ACL Strain and Cartilage Biomechanics

Complete results for correlation coefficients and P values for the parameters with strong correlations ( $\rho \geq 0.7$ ) are presented in Appendix C, Tables C1 to C5 (available online). Correlations between WB parameters and ACL strain, articular cartilage stress, and contact force are included.

TABLE 2 Final High ACL Strain Discriminators for the SLCD-D Task<sup>a</sup>

$Variable^b$	AUC	P Value	$\mathrm{Cutoff}^c$	Sensitivity	Specificity	High ACL Strain If Value Is
Kinematics						
Hip flexion	0.737	<.001	41.9	0.714	0.778	Larger
Hip adduction	0.832	<.001	-2.2	0.976	0.508	Smaller
Knee flexion	0.893	<.001	34.8	0.929	0.817	Larger
Axial compression	0.673	.001	1.5	0.881	0.429	Larger
Kinetics						
Hip rotation moment	0.759	<.001	0.2	0.762	0.722	Larger
Lumbar extension moment	0.878	<.001	0.3	0.976	0.786	Larger
ATS force	0.706	<.001	0.3	0.976	0.484	Larger
GRF-ML	0.858	<.001	-0.3	0.738	0.881	Smaller
Muscles						
Gluteus medius 1	0.657	<.001	40%	0.905	0.476	Larger
Semitendinosus	0.717	<.001	92%	0.476	0.857	Larger
Gracilis	0.651	.046	86%	0.714	0.548	Smaller
Tibialis posterior	0.568	.048	92%	0.952	0.206	Smaller
Nonstance limb side						
Erector spinae	0.861	<.001	63%	0.833	0.786	Larger
External oblique	0.880	.026	33%	0.976	0.675	Smaller

<sup>&</sup>quot;ACL, anterior cruciate ligament; ATS, anterior tibial shear; AUC, area under the curve; GRF, ground-reaction force; ML, medial-lateral; SLCD-D, single-leg cross drop-dominant stance.

### Cutoff Values for the WB High-Risk Kinetics and Kinematics

The upper quartile for relative ACL strain was 2.32%, 3.85%, 2.2%, and 3.53% for SLCD-N, SLCD-D, SLD-N, and SLD-D, respectively. After ROC analysis and multicollinearity assessment, only a few parameters were identified as statistically significant discriminants and retained for the logistic regression analyses for each WB parameter group. Tables 2 to 5 show statistically significant parameters for predicting high ACL strain trials returned from the multivariate binary logistic regressions. Overall accuracy, sensitivity, specificity, likelihood ratios, and statistical significance of the regression models are shown in Tables 6 to 9.

### DISCUSSION

This study provided an understanding of the effect of WB parameters on the ACL and articular cartilage biomechanics in 14 physically active participants. Our main hypothesis was that increased trunk lateral bending away from the stance limb, increased hip abduction, decreased ankle plantarflexion, lower force production of the lumbopelvic musculature, and higher quadriceps forces may serve as potential predictors of high ACL strain. Even though our findings generally support this hypothesis, results from the ROC analyses further suggest that the high-risk parameters identified were task dependent. Therefore, only a few of the hypothesized parameters appeared for

each task as identifiers of high ACL strain trials. Additionally, other parameters contributing to the high ACL strain trials were identified (Tables 2-5). For example, knee flexion angle was an excellent discriminator of high ACL strain trials in SLCD-N and a good discriminator in the other 3 limb task conditions. Knee flexion moment was also a good discriminator in SLCD-N, SLD-N, and SLD-D. Higher knee flexion angles and moments were indicative of higher ACL strain in these cases, which was supported by the finding of the peak ACL strains occurring in the second half of the landing phase when the knee was more flexed (Figure 4). The association of higher knee flexion angles and moments with high ACL strain trials somewhat contradicts the previous literature. 47 However, it should be noted that the flexion angles used here were from the whole landing phase at each 8-millisecond interval and not the flexion angle at IC. In contrast, peak knee flexion angle and knee flexion angle at IC were inversely correlated with peak stresses on the articular cartilage during SLCD-D, SLD-D, and SLD-N (Appendix C, available online).

Other knee parameters previously shown to increase ACL strain included knee abduction angles and moments<sup>61</sup> and larger quadriceps muscle forces during drop vertical jumps. 61 In this study, peak knee abduction moments and angles, knee abduction moments and angles at peak ACL strain and at IC, and larger vastus medialis force (SLCD-N) were additionally shown to be highly correlated with peak articular cartilage stresses and contact forces. Therefore, training programs should focus on

 $<sup>^</sup>b$ Signs: ATS force (anterior +, posterior -); axial compression (compression +, distraction -); GRF-ML (medial -, lateral +); hip adduction (abduction -, adduction +); hip flexion (extension -, flexion +); hip rotation moment (internal -, external +); knee flexion (flexion +, extension –); lumbar extension moment (flexion –, extension +).

<sup>&</sup>lt;sup>e</sup>Units: joint angles (deg), joint translations (mm), joint moments ( $N \cdot m/kg \times m$ ), joint forces and GRF (body weight), muscle forces (% peak muscle force).

TABLE 3
Final High ACL Strain Discriminators for the SLCD-N ${\sf Task}^a$

$Variable^b$	AUC	P Value	$\mathrm{Cutoff}^c$	Sensitivity	Specificity	High ACL Strain If Value Is
Kinematics						
Lumbar extension	0.743	<.001	-10.5	0.762	0.683	Smaller
Knee flexion	0.904	<.001	37.7	0.976	0.786	Larger
Kinetics						
Knee flexion moment	0.843	<.001	1.2	0.857	0.873	Larger
ITR moment	0.640	.006	0.006	0.571	0.222	Larger
ATS force	0.748	<.001	0.5	1.000	0.548	Larger
Knee compressive force	0.691	<.001	1.7	0.976	0.508	Larger
Ankle angle moment	0.659	.002	-0.7	0.810	0.500	Smaller
GRF-AP	0.687	<.001	0.3	0.810	0.571	Larger
Muscles						
Sartorius	0.713	<.001	96%	0.810	0.651	Larger
Vastus medialis	0.875	<.001	98%	0.857	0.738	Larger
Nonstance limb-side erector spinae	0.888	<.001	48%	0.952	0.778	Larger

<sup>&</sup>lt;sup>a</sup>ACL, anterior cruciate ligament; ATS, anterior tibial shear; AUC, area under the curve; GRF, ground-reaction force; AP, anterior-posterior; ITR, internal tibial rotation; SLCD-N, single-leg cross drop-nondominant stance.

	O					
$Variable^b$	AUC	P Value	$\mathrm{Cutoff}^c$	Sensitivity	Specificity	High ACL Strain If Value Is
Kinematics						
Knee flexion	0.822	<.001	35.4	0.929	0.659	Larger
Axial compression	0.696	<.001	2.4	0.905	0.397	Larger
Hip adduction	0.684	<.001	7.3	0.929	0.357	Smaller
Anterior tibial translation	0.655	.004	5.1	0.667	0.746	Larger
Hip flexion	0.608	.035	42.2	0.833	0.373	Larger
Kinetics						
GRF-ML	0.869	<.001	-0.3	0.833	0.833	Smaller
Knee flexion moment	0.852	<.001	1.0	0.976	0.738	Larger
Lumbar extension moment	0.837	<.001	0.1	0.976	0.667	Larger
Knee adduction moment	0.734	<.001	-0.7	0.881	0.603	Smaller
GRF-AP	0.620	.020	0.0	0.690	0.571	Smaller
Lumbar rotation moment	0.618	.022	-0.1	0.929	0.302	Smaller
Muscles						
Nonstance limb-side external oblique	0.784	<.001	19%	0.738	0.770	Smaller
Tensor fasciae latae	0.782	<.001	77%	0.881	0.611	Larger
Gluteus maximus 3	0.722	<.001	5%	0.881	0.548	Smaller
Stance limb-side external oblique	0.709	<.001	56%	0.905	0.429	Smaller
Medial gastrocnemius	0.677	<.001	92%	0.810	0.500	Larger
Extensor hallucis longus	0.651	.001	77%	0.738	0.548	Larger
Nonstance limb-side internal oblique	0.650	.002	73%	0.810	0.460	Smaller
Gracilis	0.638	.002	87%	0.905	0.397	Smaller
Semitendinosus	0.603	.025	74%	0.929	0.294	Larger
Tibialis posterior	0.597	.046	72%	0.881	0.317	Smaller

<sup>&</sup>lt;sup>a</sup>ACL, anterior cruciate ligament; AUC, area under the curve; GRF, ground-reaction force; AP, anterior-posterior; ML, medial-lateral; SLD-D, single-leg drop-dominant stance.

<sup>&</sup>lt;sup>b</sup>Signs: ankle angle moment (dorsiflexion –, plantarflexion +); ATS force (anterior +, posterior –); GRF-AP (posterior –, anterior +); ITR moment (external –, internal +); knee compressive force (inferior –, superior +); knee flexion (flexion +, extension –); knee flexion moment (extension –, flexion +); lumbar extension (extension –, flexion +).

 $<sup>^{</sup>c}$ Units: joint angles (deg), joint translations (mm), joint moments (N·m/kg  $\times$  m), joint forces and GRF (body weight), muscle forces (% peak muscle force).

<sup>&</sup>lt;sup>b</sup>Signs: axial compression (compression +, distraction -); GRF-AP (posterior -, anterior +); GRF-ML (medial -, lateral +); hip adduction (abduction -, adduction +); hip flexion (extension -, flexion +); knee adduction moment (adduction -, abduction +); knee flexion (flexion +, extension -); knee flexion moment (extension -, flexion +); lumbar extension moment (flexion -, extension +); lumbar rotation moment (away from the stance limb -, toward the stance limb +); tibial translation (anterior +, posterior -).

 $<sup>^{</sup>c}$ Units: joint angles (deg), joint translations (mm), joint moments (N·m/kg  $\times$  m), joint forces and GRF (body weight), muscle forces (% peak muscle force).

TABLE 5
Final High ACL Strain Discriminators for the SLD-N Task <sup>a</sup>

$Variable^b$	AUC	P Value	$\mathrm{Cutoff}^c$	Sensitivity	Specificity	High ACL Strain If Value Is
Kinematics						
Hip adduction	0.661	.001	-10.0	0.881	0.397	Larger
Knee flexion	0.810	<.001	40.7	0.905	0.746	Larger
Axial compression	0.735	<.001	2.5	0.857	0.611	Larger
Kinetics						
Hip adduction moment	0.633	.010	-0.1	0.667	0.619	Larger
Knee flexion moment	0.834	<.001	1.1	0.929	0.738	Larger
GRF-ML	0.849	<.001	-0.3	0.810	0.762	Smaller
Muscles						
Gluteus medius 1	0.703	<.001	10%	0.643	0.746	Smaller
Gluteus maximus 1	0.708	.014	1%	0.500	0.841	Smaller
Rectus femoris	0.667	<.001	98%	0.738	0.587	Larger
Tibialis anterior	0.602	.034	54%	0.762	0.508	Larger
Nonstance limb-side erector spinae	0.772	<.001	44%	0.952	0.611	Larger

<sup>&</sup>lt;sup>a</sup>ACL, anterior cruciate ligament; AUC, area under the curve; GRF, ground-reaction force; ML, medial-lateral; SLD-N, single-leg dropnondominant stance.

TABLE 6 Regression Models: SLCD-D Kinematics, Kinetics, and Muscles<sup>a</sup>

$\chi^2$	df	P Value	Nagelkerke $R^2$	
98.846	4	<.001	0.659	
90.391	4	<.001	0.616	
117.241	6	<.001	0.744	
True Negative	False Negative	False Positive	True Positive	Overall Percentage Correct
117	10	9	32	88.7
114	16	12	26	83.3
120	12	6	30	89.3
Sensitivity	Specificity	LR+	LR–	
0.762	0.929	10.667	0.256	
0.619	0.905	6.500	0.421	
0.714	0.952	15.000	0.300	
	98.846 90.391 117.241 True Negative 117 114 120 Sensitivity 0.762 0.619	98.846 4 90.391 4 117.241 6  True Negative False Negative  117 10 114 16 120 12  Sensitivity Specificity  0.762 0.929 0.619 0.905	98.846 4 <.001 90.391 4 <.001 117.241 6 <.001  True Negative False Negative False Positive  117 10 9 114 16 12 120 12 6  Sensitivity Specificity LR +  0.762 0.929 10.667 0.619 0.905 6.500	98.846 4 <.001 0.659 90.391 4 <.001 0.616 117.241 6 <.001 0.744  True Negative False Negative False Positive True Positive  117 10 9 32 114 16 12 26 120 12 6 30  Sensitivity Specificity LR + LR-  0.762 0.929 10.667 0.256 0.619 0.905 6.500 0.421

<sup>&</sup>lt;sup>a</sup>LR, likelihood ratio; SLCD-D, single-leg cross drop-dominant stance.

exercises that lead to decreasing abduction angles and moments. Furthermore, the anterior tibial shear force that was previously shown to load the ACL and increase the ACL strain<sup>34</sup> was positively correlated with ACL strain and articular cartilage stress and contact force in this work.

Larger lumbar extension moment (SLCD-D, SLD-D), larger nonstance limb-side erector spinae force (SLCD-N, SLCD-D), and smaller nonstance limb-side external oblique force (SLCD-D) were among the good discriminators of high ACL strains. These outcomes are supported by the literature: lumbar extension and spine extensor muscles that prevent lumbar flexion were previously shown to be detrimental to ACL injury.<sup>31</sup> Stronger lumbopelvic-hip muscles were shown to be protective of the knee joint by increasing trunk flexion and decreasing knee valgus and hip adduction angles during side-step cutting.32

Hip abduction and adduction moments were both identified in the literature as ACL injury risk factors,8 which supports our finding that greater hip abduction (SLCD-D, SLD-D) was associated with high ACL strains.

Lower ankle plantarflexion moments and angles and plantarflexion at IC were positively correlated with ACL strain and cartilage contact force and stress. This is supported by literature stating that ACL injury happens with flat-foot landing,<sup>5</sup> which is when ankle plantarflexion is zero. Our results also showed that gracilis and

<sup>&</sup>lt;sup>b</sup>Signs: axial compression (compression +, distraction -); GRF-ML (lateral -, medial +); hip adduction (abduction -, adduction +); hip adduction moment (adduction -, abduction +); knee flexion (flexion +, extension -); knee flexion moment (extension -, flexion +).

<sup>&</sup>lt;sup>e</sup>Units: joint angles (deg), joint translations (mm), joint moments ( $N \cdot m/kg \times m$ ), joint forces and GRF (body weight), muscle forces (% peak muscle force).

2106	Sadeqi	et	a

TABLE 7					
Regression Models: SLCD-N Kinematics, I	Kinetics,	and	$Muscles^a$		

	O .		, ,		
Model: SLCD-N	$\chi^2$	df	P Value	Nagelkerke $\mathbb{R}^2$	
Kinematic	83.852	2	<.001	0.582	
Kinetic	127.953	6	<.001	0.789	
Muscles	98.993	3	<.001	0.659	
	True Negative	False Negative	False Positive	True Positive	Overall Percentage Correct
Kinematic	116	15	10	27	85.1
Kinetic	118	9	8	33	89.9
Muscles	117	9	9	33	89.3
	Sensitivity	Specificity	LR +	LR-	
Kinematic	0.643	0.921	8.100	0.388	
Kinetic	0.786	0.937	12.375	0.229	
Muscles	0.786	0.929	11.000	0.231	

<sup>&</sup>lt;sup>a</sup>LR, likelihood ratio; SLCD-N, single-leg cross drop-nondominant stance.

TABLE 8 Regression Models: SLD-D Kinematics, Kinetics, and Muscles<sup>a</sup>

Model: SLD-D	$\chi^2$	df	P Value	Nagelkerke $\mathbb{R}^2$	
Kinematic	81.906	5	<.001	0.571	
Kinetic	121.827	6	<.001	0.764	
Muscles	136.308	10	<.001	0.823	
	True Negative	False Negative	False Positive	True Positive	Overall Percentage Correct
Kinematic	113	18	13	24	81.5
Kinetic	118	10	8	32	89.3
Muscles	120	5	6	37	93.5
	Sensitivity	Specificity	LR+	LR–	
Kinematic	0.571	0.897	5.538	0.478	
Kinetic	0.762	0.937	12.000	0.254	
Muscles	0.881	0.952	18.500	0.125	

<sup>&</sup>lt;sup>a</sup>LR, likelihood ratio; SLD-D, single-leg drop-dominant stance.

gastrocnemii muscle forces were inversely correlated with ACL strain and articular cartilage stress and contact force.

The outcomes of the FE simulation were in agreement with the previous literature. Cadaveric simulations of bipedal landings showed postimpact increases of 2.9% to 5.7% in ACL strain.<sup>2</sup> Peak values of 7% ± 4% were previously reported for in vivo ACL strain during single-leg jumps. 16 Peak ACL strains in this study were close to those in the literature, except for SLCD-D, which was higher than in modeling or in vitro studies. Higher strain values could be a result of the more challenging tasks in this study and higher ground-reaction forces in single-leg landings versus double-leg jumps. Cartilage contact forces were in agreement with previous studies,9 with peaks up to 5.72 body weight and 4.56 body weight for medial and lateral tibial cartilage, respectively. Higher contact force and pressure on the medial component were noted by other researchers. 44

Stresses in the range of 21.5  $\pm$  3.2, 20.2  $\pm$  3.4, and 23.1  $\pm$ 3.4 MPa on the patellofemoral cartilage were previously cited during normal running, running with a flexed torso, and running with an extended torso, respectively.<sup>59</sup> Tibiofemoral cartilage stresses in the range of 1.5 to 12 MPa during gait have been reported by other studies.36,64 Literature is sparse and limited in reporting tibiofemoral cartilage stress values during single-leg landings; the range of tibiofemoral stress in this study was 6.47 to 18.25 MPa across all tasks. Peak contact pressures of 8.21 MPa<sup>56</sup> and 12 to 15 MPa<sup>60</sup> were noted during normal gait. Cadaveric experiments showed mean pressure of 14 ± 4 MPa under compressive loads and 10.64 ± 6 MPa under internal rotation torque, <sup>38</sup> which support the values of pressure obtained in this work.

The 5-DOF knee joint used in this study—as opposed to the previous DOF representation of the hinge joint 45 or the modeling of the secondary DOF as prescribed functions of

Model: SLD-N	$\chi^2$	df	P Value	Nagelkerke $\mathbb{R}^2$	
Kinematic	50.621	3	<.001	0.385	
Kinetic	95.902	3	<.001	0.644	
Muscles	115.434	5	<.001	0.736	
	True Negative	False Negative	False Positive	True Positive	Overall Percentage Correct
Kinematic	114	26	12	16	77.4
Kinetic	116	13	10	29	86.3
Muscles	119	10	7	32	89.9
	Sensitivity	Specificity	LR +	LR-	
Kinematic	0.381	0.905	4.000	0.684	
Kinetic	0.690	0.921	8.700	0.336	
Muscles	0.762	0.944	13.714	0.252	

TABLE 9 Regression Models: SLD-N Kinematics, Kinetics, and Muscles<sup>a</sup>

flexion angle 12—helps in providing details on the high-risk knee motions and loads, such as abduction moments and angles, internal tibial rotation moments and angles, and anterior tibial shear force and translation.<sup>29</sup> We acknowledge the previous use of a 6-DOF knee joint model during gait<sup>6</sup> and dynamic tasks<sup>61</sup>; however, there were some simplifications in their FE simulations, which are discussed in turn. As demonstrated in our previous study, 52 ligament material properties play a significant role in knee joint biomechanics in FE simulations. So, simplifying these properties to linear spring stiffness<sup>36</sup> will not produce accurate results of the joint behavior. Other simplifications of previous FE models were the use of bundles of nonlinear 2dimensional springs for the ligaments<sup>29</sup> instead of anatomic 3-dimensional structures created by segmenting the medical images.

The FE model in this study was actuated kinetically with moments and forces for the 4 DOF of abduction/ adduction moment, tibial rotation moment, anterior tibial shear force, and knee compressive force and kinematically driven with rotations for the flexion angle. Previous literature reported moment-actuated knee models to be more accurate and complex than rotation-actuated models. 6,36 Comparing the kinetic-versus kinematic-driven knee models with data from motion analysis experiments revealed more even stress and strain distributions for the cartilage throughout the gait cycle for the kinetically actuated models.<sup>36</sup> Another study reported comparable outputs for cartilage stress and strains in the kinetic- and kinematic-driven knee joint models with the kinetically actuated simulations. In a similar study, Ueno et al used motion analysis, musculoskeletal simulations, FE, and logistic regressions to predict high ACL strain trials. However, they analyzed a different task, the drop vertical jump, with the focus being mainly on ACL strains and loads, whereas in the current study, we simulated single-leg landings, and in addition to ACL strain, we investigated the association of WB parameters with cartilage contact forces and stress.

### Limitations

Only 1 joint geometry was used in the FE simulations; using the magnetic resonance imaging of the same participants who were doing the motion analysis experiments for the FE models<sup>36</sup> would lead to more accurate results. The mediolateral translation was fixed in the models, and just 5 of the 6 knee joint DOF were modeled in the FE simulations. This is a limitation of this study because mediolateral motion occurs at the normal knee joint<sup>4</sup> and can affect the outcomes of ROC and logistic regressions. Yet, many of the previous studies modeled the knee as a hinge joint or allowed for only the 3 rotations or 4 DOF. A previous study from our laboratory reported the highest ACL strains to happen during multiplanar loadings of knee abduction moment, internal tibial rotation moment, and anterior tibial shear force combined with axial impact with the knee in  $25^{\circ}$ of flexion<sup>34</sup>: therefore, we included these 5 DOF in the model and locked the mediolateral translation for simplification. Future works may include this DOF during SLD and SLCD simulations and compare the outcomes with the results of this work. Additionally, the full body model used in this study did not include the arms (left and right humerus, ulna, radius, and hand), and this would affect the overall optimization results in the static optimizations, leading to differences between the calculated muscle forces and the actual anatomic muscle forces. Another limitation of this work was the small sample size (14 participants). which makes it difficult to generalize the results. Additionally, the participants were not athletes, and their unfamiliarity with the tasks could affect their performance in terms of technique, muscle activations, and muscle fatigue. 21 Another factor that could count as a limitation is pooling both sexes. It is likely that the regression models would have higher accuracies for just a single sex owing to the sex differences in landing biomechanics and sex-specific injury mechanisms.  $^{48,49}$  However, combining the landing biomechanics for the sexes can lead to more generalized recommendations.

<sup>&</sup>lt;sup>a</sup>LR, likelihood ratio; SLD-N, single-leg drop-nondominant stance.

### CONCLUSION

Investigation of the effect of WB parameters on ACL and articular cartilage biomechanics during SLCD and SLD demonstrated trunk, lumbopelvic, hip, knee, and ankle parameters affecting ACL strain and articular cartilage stress and contact forces. Factors that were collectively detrimental to ACL and articular cartilage during the 4 analyzed tasks and should be minimized during single-leg landings include higher peak knee abduction moments and angles, greater knee abduction moments and angles at IC, lower ankle plantarflexion moments and angles, lower plantarflexion at IC, larger peak anterior tibial shear force, lower gracilis muscle force, lower gluteus maximus muscle force, and lower gastrocnemii muscle force. These outcomes can be used in developing ACL injury prevention training programs.

#### **ACKNOWLEDGMENT**

The authors thank Dave Sherman, Kassondra Verhoff, Cody Zink, Matthew Barnett, and Kandalyn Noe for their contributions to data collection. The authors also thank Dr Timothy Hewett, Mayo Clinic, and his coworkers for providing the computed tomography and magnetic resonance imaging scans of the knees and the results of their cadaveric study that were used to validate our FE models.

### **ORCID iD**

Sara Sadeqi https://orcid.org/0000-0003-0353-9661

### **REFERENCES**

- Adouni M, Shirazi-Adl A, Shirazi R. Computational biodynamics of human knee joint in gait: from muscle forces to cartilage stresses. J Biomech. 2012;45(12):2149-2156.
- Bates NA, Schilaty ND, Krych AJ, Hewett TE. Variation in ACL and MCL strain before initial contact is dependent on injury risk level during simulated landings. Orthop J Sports Med. 2019;7(11):2325967119884906.
- Bates NA, Schilaty ND, Nagelli CV, Krych AJ, Hewett TE. Novel mechanical impact simulator designed to generate clinically relevant anterior cruciate ligament ruptures. Clin Biomech (Bristol, Avon). 2017;44:36-44
- Belvedere C, Leardini A, Giannini S, Ensini A, Bianchi L, Catani F. Does medio-lateral motion occur in the normal knee? An in-vitro study in passive motion. *J Biomech*. 2011;44(5):877-884.
- Boden BP, Torg JS, Knowles SB, Hewett TE. Video analysis of anterior cruciate ligament injury: abnormalities in hip and ankle kinematics. Am J Sports Med. 2009;37(2):252-259.
- Bolcos PO, Mononen ME, Mohammadi A, et al. Comparison between kinetic and kinetic-kinematic driven knee joint finite element models. Sci Rep. 2018;8(1):17351.
- Cannon J, Cambridge ED, McGill SM. Increased core stability is associated with reduced knee valgus during single-leg landing tasks: investigating lumbar spine and hip joint rotational stiffness. J Biomech. 2021:116:110240.
- Chaudhari AM, Andriacchi TP. The mechanical consequences of dynamic frontal plane limb alignment for non-contact ACL injury. J Biomech. 2006;39(2):330-338.

- 9. Costigan PA, Deluzio KJ, Wyss UP. Knee and hip kinetics during normal stair climbing. *Gait Posture*. 2002;16(1):31-37.
- Critchley ML, Davis DJ, Keener MM, et al. The effects of mid-flight whole-body and trunk rotation on landing mechanics: implications for anterior cruciate ligament injuries. Sports Biomech. 2020;19(4): 421-437
- 11. Crowninshield RD, Brand RA. A physiologically based criterion of muscle force prediction in locomotion. *J Biomech.* 1981;14(11): 793-801.
- Delp SL, Anderson FC, Arnold AS, et al. OpenSim: open-source software to create and analyze dynamic simulations of movement. *IEEE Trans Biomed Eng.* 2007;54(11):1940-1950.
- Dempsey AR, Elliott BC, Munro BJ, Steele JR, Lloyd DG. Whole body kinematics and knee moments that occur during an overhead catch and landing task in sport. Clin Biomech (Bristol, Avon). 2012;27(5):466-474.
- DiCesare CA, Bates NA, Barber Foss KD, et al. Reliability of 3-dimensional measures of single-leg cross drop landing across 3 different institutions: implications for multicenter biomechanical and epidemiological research on ACL injury prevention. Orthop J Sports Med. 2015;3(12):2325967115617905.
- Donnelly CJ, Lloyd DG, Elliott BC, Reinbolt JA. Optimizing wholebody kinematics to minimize valgus knee loading during sidestepping: implications for ACL injury risk. *J Biomech*. 2012;45(8):1491-1497.
- Englander ZA, Lau BC, Wittstein JR, Goode AP, DeFrate LE. Patellar tendon orientation and strain are predictors of ACL strain in vivo during a single-leg jump. Orthop J Sports Med. 2021;9(3):232596712199 1054.
- Erbulut DU, Sadeqi S, Summers R, Goel VK. Tibiofemoral cartilage contact pressures in athletes during landing: a dynamic finite element study. J Biomech Eng. 2021;143(10):101006.
- Fleming BC, Beynnon BD, Tohyama H, et al. Determination of a zero strain reference for the anteromedial band of the anterior cruciate ligament. J Orthop Res. 1994;12(6):789-795.
- Frank B, Bell DR, Norcross MF, Blackburn JT, Goerger BM, Padua DA. Trunk and hip biomechanics influence anterior cruciate loading mechanisms in physically active participants. Am J Sports Med. 2013;41(11):2676-2683.
- Gagnier JJ, Morgenstern H, Chess L. Interventions designed to prevent anterior cruciate ligament injuries in adolescents and adults: a systematic review and meta-analysis. Am J Sports Med. 2013;41(8):1952-1962.
- Gehring D, Melnyk M, Gollhofer A. Gender and fatigue have influence on knee joint control strategies during landing. *Clin Biomech* (Bristol, Avon). 2009;24(1):82-87.
- Gottlob C, Baker C Jr. Anterior cruciate ligament reconstruction: socioeconomic issues and cost effectiveness. Am J Orthop (Belle Mead NJ). 2000;29(6):472-476.
- Halonen KS, Mononen ME, Jurvelin JS, et al. Importance of patella, quadriceps forces, and depthwise cartilage structure on knee joint motion and cartilage response during gait. *J Biomech Eng*. 2016;138(7):071002. doi:10.1115/1.4033516
- Hewett TE, Lindenfeld TN, Riccobene JV, Noyes FR. The effect of neuromuscular training on the incidence of knee injury in female athletes: a prospective study. Am J Sports Med. 1999;27(6):699-706
- Hewett TE, Myer GD, Ford KR, et al. Biomechanical measures of neuromuscular control and valgus loading of the knee predict anterior cruciate ligament injury risk in female athletes: a prospective study. Am J Sports Med. 2005;33(4):492-501.
- Hewett TE, Myer GD, Ford KR, Paterno MV, Quatman CE. Mechanisms, prediction, and prevention of ACL injuries: cut risk with three sharpened and validated tools. *J Orthop Res.* 2016;34(11):1843-1855.
- Hicks JL, Uchida TK, Seth A, Rajagopal A, Delp SL. Is my model good enough? Best practices for verification and validation of musculoskeletal models and simulations of movement. *J Biomech Eng*. 2015;137(2):020905.

- 28. Huang Y-L, Jung J, Mulligan CM, Oh J, Norcross MF. A majority of anterior cruciate ligament injuries can be prevented by injury prevention programs: a systematic review of randomized controlled trials and cluster-randomized controlled trials with meta-analysis. Am J Sports Med. 2020;48(6):1505-1515.
- 29. Hume DR, Navacchia A, Rullkoetter PJ, Shelburne KB. A lower extremity model for muscle-driven simulation of activity using explicit finite element modeling. J Biomech. 2019;84:153-160.
- 30. Ithurburn MP. Paterno MV. Ford KR. Hewett TE. Schmitt LC. Young athletes with quadriceps femoris strength asymmetry at return to sport after anterior cruciate ligament reconstruction demonstrate asymmetric single-leg drop-landing mechanics. Am J Sports Med. 2015;43(11):2727-2737.
- 31. Jamison ST, McNally MP, Schmitt LC, Chaudhari AM. The effects of core muscle activation on dynamic trunk position and knee abduction moments: implications for ACL injury. J Biomech. 2013;46(13):2236-
- 32. Jeong J, Choi D-H, Shin CS. Core strength training can alter neuromuscular and biomechanical risk factors for anterior cruciate ligament injury. Am J Sports Med. 2021;49(1):183-192.
- 33. Kagaya Y, Fujii Y, Nishizono H. Association between hip abductor function, rear-foot dynamic alignment, and dynamic knee valgus during single-leg squats and drop landings. J Sport Health Sci. 2015;4(2):182-187.
- 34. Kiapour AM. Demetropoulos CK. Kiapour A. et al. Strain response of the anterior cruciate ligament to uniplanar and multiplanar loads during simulated landings: implications for injury mechanism. Am J Sports Med. 2016;44(8):2087-2096.
- 35. Kingston B, Murray A, Norte GE, Glaviano NR. Validity and reliability of 2-dimensional trunk, hip, and knee frontal plane kinematics during single-leg squat, drop jump, and single-leg hop in females with patellofemoral pain. Phys Ther Sport. 2020;45:181-187.
- 36. Kłodowski A, Mononen ME, Kulmala JP, et al. Merge of motion analysis, multibody dynamics and finite element method for the subjectspecific analysis of cartilage loading patterns during gait: differences between rotation and moment-driven models of human knee joint. Multibody Syst Dyn. 2016;37(3):271-290.
- 37. Menzer H, Slater LV, Diduch D, et al. The utility of objective strength and functional performance to predict subjective outcomes after anterior cruciate ligament reconstruction. Orthop J Sports Med. 2017:5(12):2325967117744758.
- 38. Meyer EG, Baumer TG, Slade JM, Smith WE, Haut RC. Tibiofemoral contact pressures and osteochondral microtrauma during anterior cruciate ligament rupture due to excessive compressive loading and internal torque of the human knee. Am J Sports Med. 2008:36(10):1966-1977.
- 39. Mokhtarzadeh H, Perraton L, Fok L, et al. A comparison of optimisation methods and knee joint degrees of freedom on muscle force predictions during single-leg hop landings. J Biomech. 2014;47(12):2863-2868.
- 40. Myer GD, Bates NA, DiCesare CA, et al. Reliability of 3-dimensional measures of single-leg drop landing across 3 institutions: implications for multicenter research for secondary ACL-injury prevention. J Sport Rehabil. 2015;24(2):198-209.
- 41. Navacchia A, Bates NA, Schilaty ND, Krych AJ, Hewett TE. Knee abduction and internal rotation moments increase ACL force during landing through the posterior slope of the tibia. J Orthop Res. 2019;37(8):1730-1742.
- 42. Oliphant TE. Python for scientific computing. Comp Sci Eng. 2007;9(3):10-20.
- 43. Olsen O-E, Myklebust G, Engebretsen L, Bahr R. Injury mechanisms for anterior cruciate ligament injuries in team handball: a systematic video analysis. Am J Sports Med. 2004;32(4):1002-1012.
- 44. Park S, Lee S, Yoon J, Chae S-W. Finite element analysis of knee and ankle joint during gait based on motion analysis. Med Eng Phys. 2019:63:33-41.

- 45. Peel SA. Schroeder LE. Weinhandl JT. Lower extremity muscle contributions to ACL loading during a stop-jump task. J Biomech. 2021:121:110426.
- 46. Pflum MA, Shelburne KB, Torry MR, Decker MJ, Pandy MG. Model prediction of anterior cruciate ligament force during drop-landings. Med Sci Sports Exerc. 2004;36(11):1949-1958.
- 47. Pollard CD, Sigward SM, Powers CM. Limited hip and knee flexion during landing is associated with increased frontal plane knee motion and moments. Clin Biomech (Bristol, Avon), 2010;25(2):142-146.
- 48. Quatman CE, Ford KR, Myer GD, Hewett TE. Maturation leads to gender differences in landing force and vertical jump performance: a longitudinal study. Am J Sports Med. 2006;34(5):806-813.
- 49. Quatman CE, Hewett TE. The anterior cruciate ligament injury controversy: is "valgus collapse" a sex-specific mechanism? Br J Sports Med. 2009;43(5):328-335.
- 50. Quatman CE, Quatman-Yates CC, Hewett TE. A "plane" explanation of anterior cruciate ligament injury mechanisms. Sports Med. 2010;40(9):729-746.
- 51. Roelker SA, Caruthers EJ, Hall RK, Pelz NC, Chaudhari AMW, Siston RA. Effects of optimization technique on simulated muscle activations and forces. J Appl Biomech. 2020;36(4):259-278.
- 52. Sadeqi S, Summers R, Erbulut DU, Goel VK. Optimization of material coefficients in the Holzapfel-Gasser-Ogden material model for the main four ligaments of the knee joint - a finite element study. Applied Mathematics. 2021;12(12):1166-1188.
- 53. Schmitt LC, Paterno MV, Ford KR, Myer GD, Hewett TE. Strength asymmetry and landing mechanics at return to sport after ACL reconstruction. Med Sci Sports Exerc. 2015;47(7):1426.
- 54. Sherman D, Birchmeier T, Kuenze CM, et al. Thigh-muscle and patient-reported function early after anterior cruciate ligament reconstruction: clinical cutoffs unique to graft type and age. J Athl Train. 2020:55(8):826-833.
- 55. Shin CS. Chaudhari AM. Andriacchi TP. The influence of deceleration forces on ACL strain during single-leg landing: a simulation study. J Biomech. 2007;40(5):1145-1152.
- 56. Shu L, Yamamoto K, Yoshizaki R, Yao J, Sato T, Sugita N. Multiscale finite element musculoskeletal model for intact knee dynamics. Comput Biol Med. 2022;141:105023.
- 57. Stanev D, Moustakas K, Gliatis J, Koutsojannis C. ACL reconstruction decision support. Methods Inf Med. 2016;55(1):98-105.
- 58. Tanska P, Mononen ME, Korhonen RK. A multi-scale finite element model for investigation of chondrocyte mechanics in normal and medial meniscectomy human knee joint during walking. J Biomech. 2015;48(8):1397-1406.
- 59. Teng H-L, Powers CM. Sagittal plane trunk posture influences patellofemoral joint stress during running. J Orthop Sports Phys Ther. 2014;44(10):785-792.
- 60. Thambyah A, Goh JC, De SD. Contact stresses in the knee joint in deep flexion. Med Eng Phys. 2005;27(4):329-335.
- 61. Ueno R, Navacchia A, Schilaty ND, Myer GD, Hewett TE, Bates NA. Anterior cruciate ligament loading increases with pivot-shift mechanism during asymmetrical drop vertical jump in female athletes. Orthop J Sports Med. 2021;9(3):2325967121989095.
- 62. Weber P, Woiczinski M, Steinbrück A, et al. Increase in the tibial slope in unicondylar knee replacement: analysis of the effect on the kinematics and ligaments in a weight-bearing finite element model. Biomed Res Int. 2018:2018:8743604.
- 63. Withrow TJ, Huston LJ, Wojtys EM, Ashton-Miller JA. The relationship between quadriceps muscle force, knee flexion, and anterior cruciate ligament strain in an in vitro simulated jump landing. Am J Sports Med. 2006;34(2):269-274.
- 64. Yang NH, Nayeb-Hashemi H, Canavan PK, Vaziri A. Effect of frontal plane tibiofemoral angle on the stress and strain at the knee cartilage during the stance phase of gait. J Orthop Res. 2010;28(12):1539-1547.